

A New Route to Highly Stretchable and Soft Inorganic–Organic Hybrid Elastomers Using Polydimethylsiloxane as Crosslinker of Epoxidized Natural Rubber

Shib Shankar Banerjee,* Susanta Banerjee, Sven Wießner, Andreas Janke, Gert Heinrich, and Amit Das*

Sulfur or peroxide crosslinking is the most common and conventional method to develop elastomeric materials. A new approach to crosslink epoxidized natural rubber (ENR) by aminopropyl terminated polydimethylsiloxane (AT-PDMS) is described, intending to develop a new kind of hybrid organic–inorganic elastomers. The curing reaction is accelerated by using hydroquinone as a catalyst. The formation of the hybrid structure is evident from the appearance of two glass transition temperatures, at -1 and -120 °C, for the ENR and PDMS phases, respectively. The curing reaction is found to be of first order with respect to amine concentration with the estimated activation energy of ≈ 62 kJ mol $^{-1}$. Comparing the mechanical properties to a typical ENR-sulfur system leads to the conclusion that the ENR/AT-PDMS hybrid structure is highly stretchable and soft, as demonstrated by its relatively higher strain at failure (up to $\approx 630\%$), and lower hardness and modulus values. The higher stretchability and soft nature of the material are achieved by introducing flexible PDMS chains during the curing process resulting to a hybrid elastomer networks. This kind of soft but robust materials can find several applications in diverse fields, such as soft robotics, flexible, and stretchable electronics.

Like NR, ENR can also undergo strain-induced crystallization resulting in superior tensile and fatigue properties.^[6] ENR is highly polar, and it exhibits enhanced compatibility with polymers having polar groups like polyamide, carboxylated nitrile rubber, or poly(vinyl chloride).^[7–9] The dual functionality of ENR, namely, epoxy functional groups and double bonds are both available for crosslinking. Although sulfur vulcanization is an efficient crosslinking system, its ageing resistance is low as compared with peroxide crosslinked system. However, some mechanical properties of peroxide vulcanizates, such as tensile strength, dynamic properties, and ageing properties are inferior to sulfur vulcanizates.^[10] Alternatively, ENR can be crosslinked via the epoxy-functional group with other polyfunctional chemicals, such as dibasic acids and polyamines, and electron beam radiation.^[11–15] Epoxide group in ENR can also react with monofunctional curative. The exploration of epoxide groups as a site for crosslinking may lead to the

development of some new properties and applications of the ENR based composites. Additionally, it can provide an alternative vulcanization route to the already existing classical sulfur-vulcanization system.

1. Introduction

Epoxidized natural rubber (ENR) is a unique elastomeric material that retains most of the properties shown by natural rubber (NR) with superior oil resistance and gas-barrier properties.^[1–5]

S. S. Banerjee, S. Wießner, A. Janke, A. Das
 Leibniz-Institut für Polymerforschung Dresden e. V
 Hohe Straße 6, 01069 Dresden, Germany
 E-mail: ssbanerjee@mse.iitd.ac.in; das@ipfdd.de

S. S. Banerjee
 Department of Materials Science and Engineering
 Indian Institute of Technology Delhi
 Hauz Khas, New Delhi 110016, India

S. Banerjee
 Materials Science Centre
 Indian Institute of Technology Kharagpur
 Kharagpur 721302, India

S. Wießner
 Institut für Werkstoffwissenschaft
 Technische Universität Dresden
 D-01069 Dresden, Germany

G. Heinrich
 Institut für Textilmaschinen und Textile Hochleistungswerkstofftechnik
 Technische Universität Dresden
 Hohe Straße 6, 01069 Dresden, Germany

 The ORCID identification number(s) for the author(s) of this article can be found under <https://doi.org/10.1002/mame.202100380>

© 2021 The Authors. Macromolecular Materials and Engineering published by Wiley-VCH GmbH. This is an open access article under the terms of the Creative Commons Attribution License, which permits use, distribution and reproduction in any medium, provided the original work is properly cited.

DOI: 10.1002/mame.202100380

Polydimethylsiloxane (PDMS) is one of the most versatile and interesting polymers due to its unique properties such as low glass transition temperature, very high chain flexibility, transparency, high hydrophobicity, biocompatibility, excellent thermal stability, and dielectric properties.^[16,17] Therefore, it is possible to impart such functional properties to the polymer or polymeric system into which it is incorporated or reacted. However, very low surface energy and nonpolar nature, with low levels of intermolecular attractions enable PDMS thermodynamically and mechanically incompatible with most organic polymers.^[18] This is evident from its very low solubility parameter ($15.3 \text{ J}^{1/2} \cdot \text{cm}^{3/2}$) as compared to other polymers ($17.6\text{--}28.6 \text{ J}^{1/2} \cdot \text{cm}^{3/2}$).^[19] Therefore, reaction or incorporation of PDMS with other polymers is difficult, especially considering the polarity difference between the two polymers. Such difficulties can be overcome by introducing terminal functional group in the PDMS chains, which can lead to enhanced compatibility and reactivity with other polymers. In the present work, a very low molecular weight aminopropyl terminated PDMS (AT-PDMS) was used as a chemical crosslinker for ENR. The amine group of AT-PDMS can react with the epoxy group of ENR to develop a soft hybrid elastomeric network, thus generating a possible route of epoxy-amine curing reaction involving a nucleophilic attack of the amine nitrogen on the terminal carbon of the epoxy-functional group.^[20] A primary amine can react twice with the epoxy group in such reactions, while a secondary amine can react only once.^[20] This reaction is generally catalyzed by hydroxyl groups or by other catalytic impurities.^[21] In this work, hydroquinone was used as a catalyst.

Soft elastomeric materials have drawn significant attention because of their widespread applications in diverse fields, such as soft robotics, flexible and stretchable electronics, flexible sensors and actuators, soft coatings, and also in biology.^[22–24] In most of the technological application of soft materials, generally very crude raw material like liquid PDMS or polyurethane is used. There are few commercially available natural and synthetic elastomers which have wide applications in tire and rubber industries. However, these rubbers generally are not being used in soft materials technology due to lack of adequate softness and functionality. In this work, for the first time, an attempt has been made to develop soft functional elastomeric materials by curing of ENR rubber with AT-PDMS. Our current investigation focuses on the curing of ENR with low molecular weight AT-PDMS catalyzed by hydroquinone employing the standard elastomer processing techniques. The curing behavior, tensile properties, and dynamic mechanical properties of the ENR/AT-PDMS hybrid structure are investigated.

2. Experimental Section

2.1. Materials

ENR having 50 mol % epoxidic units (ENR 50) was obtained from Thailand, Prince of Songkla University, Surat Thani. AT-PDMS number average molecular weight 875 g mol^{-1} ; density 0.98 g cm^{-3} was procured from Sigma Aldrich. Hydroquinone (99%), sulfur, zinc oxide, stearic acid, and vulcanizing accelerator *N*-tert-butyl-2-benzothiazyl sulphonamide (TBBS) were also purchased from Sigma Aldrich and used without further purification. Fumed silica (ULTRASIL VN 3) was obtained from Evonik

with specific surface area of $180 \text{ m}^2 \text{ g}^{-1}$. Fumed silica was used in this study to disperse the liquid AT-PDMS into the rubber compound. Chemical structure of ENR, AT-PDMS, and hydroquinone are shown in **Figure 1**.

2.2. Preparation and Characterization of Samples

The mixing of the rubber compounds was carried out in three stages. In the first stage, silica/AT-PDMS/hydroquinone masterbatches were prepared. In the second stage, the compounding of ENR with this master batch was done using an internal mixer (Thermo Electron GmbH, Karlsruhe). The mixing was done at $60 \text{ }^\circ\text{C}$ for 10 min with a rotor speed of 60 rpm. The resulting compound was further mixed using a laboratory-sized two-roll mill (Polymix 110L, size: $203 \times 102 \text{ mm}^2$, Servitech GmbH, Wustermark, Germany) with a friction ratio of 1:1.2 at $40 \text{ }^\circ\text{C}$ for 5 min. The curing of the final rubber compounds was done isothermally in four different temperatures (150, 160, 170, and $180 \text{ }^\circ\text{C}$) in a hot press until their optimum curing time (t_{c90}). For comparison, sulfur curing of a typical sulfur compound of ENR was performed at $160 \text{ }^\circ\text{C}$.

2.2.1. Curing Study

Curing of ENR/AT-PDMS systems was carried out using a Rubber Process Analyzer (SIS V-50, Scarabeus GmbH, Germany) in an isothermal time sweep mode at $180 \text{ }^\circ\text{C}$ for 60 min with a frequency of 1.67 Hz. To study the kinetics of the optimized composition, samples were placed in the rheometer at four different temperatures, 150, 160, 170, and $180 \text{ }^\circ\text{C}$ for 60 min.

2.2.2. Swelling Study

To analyze the network structure of the ENR/AT-PDMS vulcanizates, swelling test was performed and the crosslink density was measured. Toluene was used here as solvent. Pre-weighed specimens were swollen for 72 h at $20 \text{ }^\circ\text{C}$ and the solvent was replaced with fresh solvent batches from time to time. The equilibrium swelling was obtained from Flory–Rehner equation:^[25]

$$\nu = -\frac{\ln(1 - V_r) + V_r + \chi V_r^2}{V_s \left(V_r^{1/3} - 0.5 V_r \right)} \quad (1)$$

where ν is the cross-link density of the rubber network, V_r is the volume fraction of the swollen rubber, χ is the Flory–Huggins interaction parameter (0.393 for ENR-Toluene),^[26] and V_s is the molar volume of solvent ($106.1 \text{ cc mol}^{-1}$ for toluene).^[26]

Volume fraction V_r was calculated based on the equation as given below:

$$V_r = \frac{[(W_d - W_f)/\rho]}{[(W_d - W_f)/\rho] + [(W_s - W_d)/\rho_s]} \quad (2)$$

where W_d , W_f , and W_s are the weight of the specimen after swelling and drying, weight of the non-extractable filler in the specimen, and the weight of the swollen specimen, respectively. ρ and ρ_s are the density of the specimen and solvent, respectively.

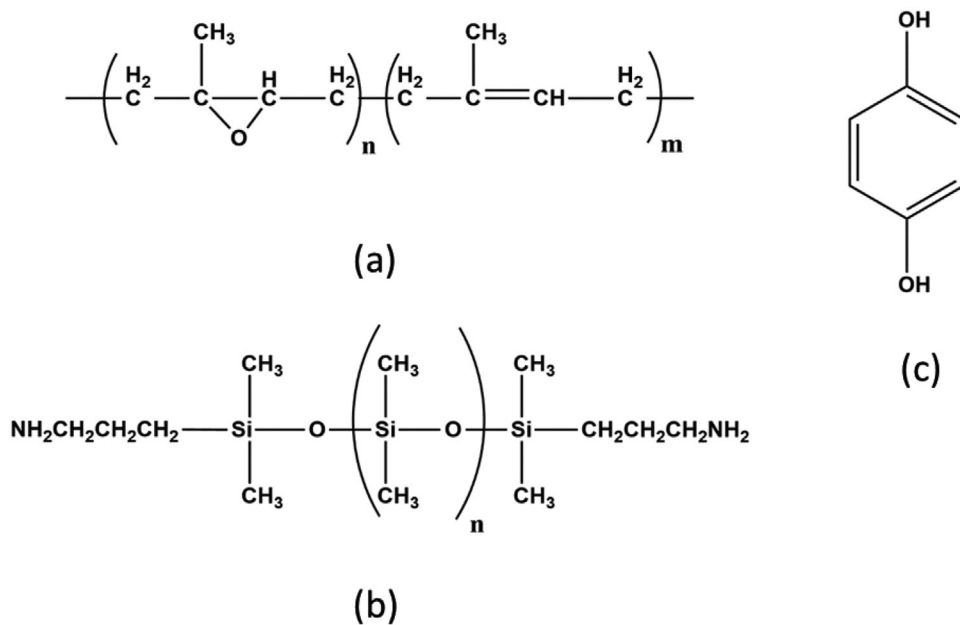


Figure 1. Chemical structure of a) ENR, b) aminopropyl terminated PDMS (AT-MDMS), and c) hydroquinone

2.2.3. Fourier Transform Infrared Spectroscopy

Fourier Transform Infrared (FTIR; in ATR mode) was carried out on a Bruker Vertex Fourier transform infrared 80 V spectrometer over the mid-IR wavenumber range 400–4000 cm⁻¹ with a 4 cm⁻¹ resolution.

2.2.4. Temperature Scanning Stress Relaxation

An instrument from Brabender GmbH, Duisburg, Germany, was used for non-isothermal relaxation measurements.^[27] Initially 50% strain was applied to the sample at 23 °C for 2 h and then the non-isothermal measurement was carried out up to 200 °C with a heating rate of 2 K min⁻¹.

2.2.5. Uniaxial Tensile Tests

Uniaxial tensile tests of all samples were performed using a mechanical testing machine (Zwick, Model No. Z010, Ulm, Germany) at room temperature at a crosshead speed of 200 mm min⁻¹.

Uniaxial cyclic tensile experiments were carried out by stretching the samples for three cycles with different strains of 50%, 100%, and 150% and then finally were stretched up to the failure.

2.2.6. Dynamic Mechanical Testing

Dynamic mechanical properties were measured in tension mode using an Eplexor 2000 N dynamic mechanic thermic spectrometer (DMTS, GABO Eplexor 2000 N). Storage modulus (*E'*), loss modulus (*E''*), and loss factor (*tanδ*) were measured and estimated from -100 to +100 °C at a heating rate of 2 K min⁻¹ using an isochronal frequency of 10 Hz.

Frequency master curves were obtained using time-temperature superposition (TTS) after measuring a combined frequency/sweep experiments from -100 to +100 °C and 0.5 to 30 Hz. The measured frequency curves were horizontally shifted using a set reference temperature of 20 °C and the master curves were reconstructed using the master curve software-module of the Eplexor-DMTS.

2.2.7. Morphology

The dispersion of fumed silica in the ENR matrix was investigated using atomic force microscopy (AFM, Bruker-Nano Inc., Santa Barbara, CA). The ultrathin sections of the samples were prepared by ultramicrotomy (Leica Ultracut UCT) at -100 °C for the AFM measurements. The experiments were conducted in a tapping mode at room temperature with a cantilever having tip radius (*r*) and spring constant of 8 nm and 40 N m⁻¹, respectively.

3. Results and Discussion

Formulations of the ENR/AT-PDMS with hydroquinone are shown in **Table 1**. The progress of ENR curing reactions via the epoxy group present in the rubber with AT-PDMS is illustrated by a plot of torque value as a function of time in **Figure 2a**. The torque curve with only AT-PDMS as a curing agent is almost flat indicating no curing reaction or formation of negligible degree of crosslink network (Figure S1). Therefore, AT-PDMS alone is not an effective curing agent for ENR and probably, a catalyst is required for the curing reaction. On the other hand, the ENR cure curve with only hydroquinone showed a slight increment of torque value suggesting formation of moderate crosslinked networks (Figure S1). In this case, ring opening of ENR is probably involved with the curing reaction as shown in **Figure 3a**.

Table 1. Formulations of ENR/AT-PDMS system with various amounts of AT-PDMS at a constant loading of HQ.

Sample No.	ENR-50	Silica	Amino propyl terminated PDMS (AP)	Hydroquinone (HQ)	Abbreviation
1.	100	15	10	–	ENR-AP ₁₀
2.	100	15	–	10	ENR-HQ ₁₀
3.	100	15	2.5	10	ENR-AP _{2.5} -HQ ₁₀
4.	100	15	5	10	ENR-AP ₅ -HQ ₁₀
5.	100	15	10	10	ENR-AP ₁₀ -HQ ₁₀
6.	100	15	20	10	ENR-AP ₂₀ -HQ ₁₀
7.	100	15	30	10	ENR-AP ₃₀ -HQ ₁₀

One control compounds are prepared; i) 100 phr ENR, 15 phr Silica, 2 phr Sulfur, 1 phr TBBS, 3 phr ZnO, 2 phr Stearic acid. This sample is designated as ENR-S.

Interestingly, a synergistic effect of curing reaction was observed from the torque value when AT-PDMS and hydroquinone were mixed with ENR (Figure 2a). At a fixed amount of hydroquinone (10 phr), the torque was found to increase up to 20 phr AT-PDMS loading and then decreased at higher loading. The high reactivity of AT-PDMS in presence of hydroquinone is probably originated

from enhanced nucleophilicity of amine group when catalyzed by hydroquinone. The carbons in the epoxide group are highly reactive electrophile to react with a strong nucleophile, like amine, carboxylic acid, alcohol, dibutylphosphate, and phosphoric acid derivatives.^[28,29] The epoxy-amine curing reaction involves a nucleophilic attack of the amine nitrogen on the terminal carbon of the epoxy functional group. Such reactions are generally catalyzed by hydroxyl groups or by any other catalytic impurities.^[21] In such reactions, a primary amine can react twice while a secondary amine can react only once with an epoxy group.^[20] The probable mechanism of curing of ENR with AT-PDMS catalyzed by hydroquinone is shown in Figure 3b.

The extent of degree of cure was estimated from the torque-time curve at different temperatures, 150, 160, 170, and 180 °C. The absolute value of torque was found to increase with increasing temperature, suggesting higher degree of crosslinking (Figure 2b). The apparent activation energy (E_a) for the curing of the ENR/AT-PDMS compounds was determined from cure curves obtained from different temperatures ranging from 150 to 180 °C. The cure rate beyond the scorch period can be written in terms of torque (Q) as a function of time (t) as:^[14]

$$dQ/dt = C (-d[A]/dt) = Ck[B]^l[E]^m[A]^n \quad (3)$$

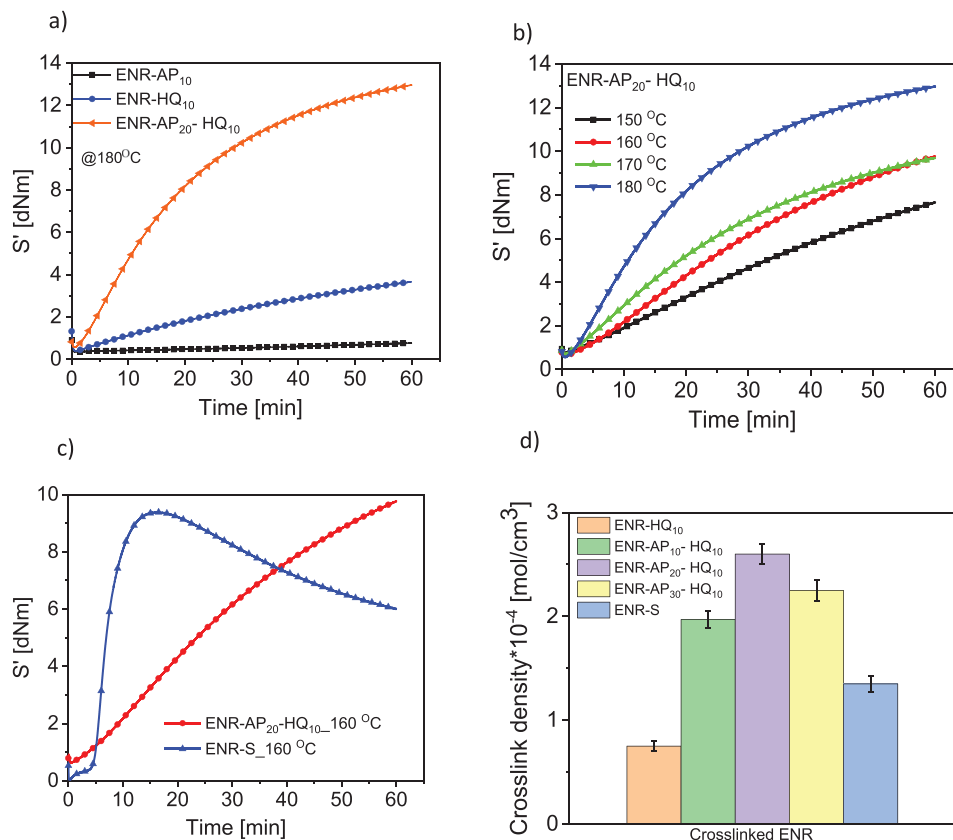


Figure 2. a) Development of real value of torque (S') with time during curing study by a Rubber Process Analyzer at 180 °C for ENR/AT-PDMS system, ENR-HQ system, and ENR/AT-PDMS-HQ system. b) Torque versus time of optimum ENR/AT-PDMS system at four different temperatures (150, 160, 170, and 180 °C), respectively. c) Comparison of torque of optimum ENR/AT-PDMS system (ENR/15Si/10HQ/20AT-PDMS) with a typical ENR-sulfur system. d) Crosslink density of different ENR vulcanizates.

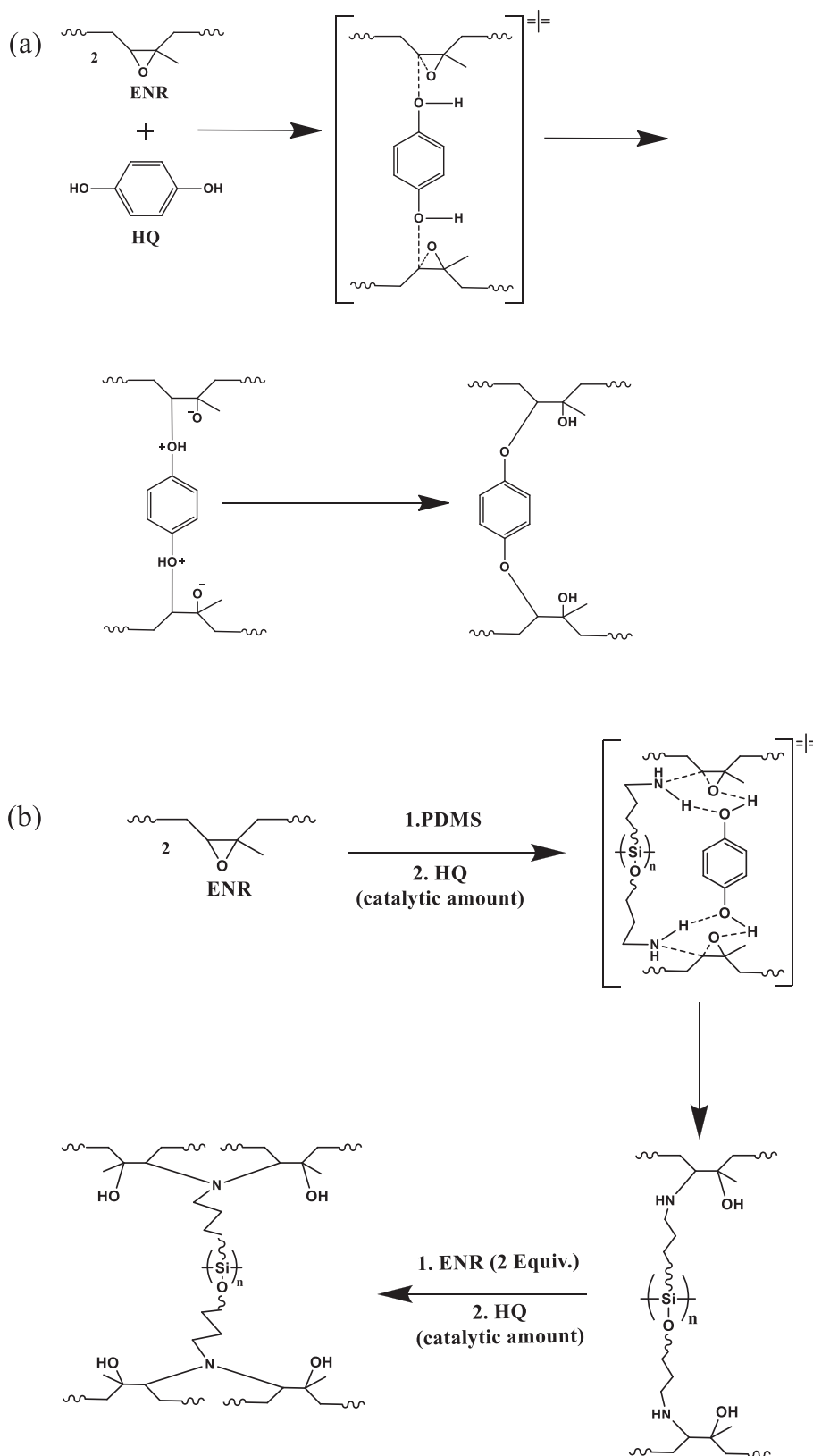


Figure 3. a) Probable scheme of ring opening reaction of ENR with hydroquinone, b) probable scheme of ring opening reaction of ENR with amino propyl terminated polydimethylsiloxane (AT-PDMS) catalyzed by hydroquinone. The hydroquinone acted not only as a catalyst, but also as a curative for ENR to some extent.

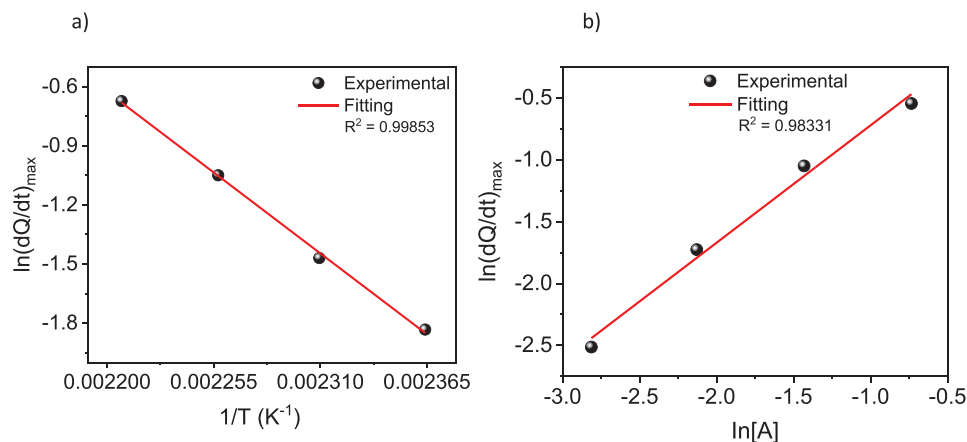


Figure 4. ENR/10HQ/20AT-PDMS composition. a) $\ln dQ/dt_{\max}$ versus $1/T$. b) $\ln (dQ/dt)_{\max}$ versus $\ln [A]$. Here, Q is the torque and $[A]$ is the amine concentration.

where k is the reaction rate constant and C is a proportionality constant. $[B]$, $[E]$, and $[A]$ are the hydroquinone, epoxide, and amine concentration, respectively and l , m , and n are the respective orders of the reactants.

The apparent activation energy according to Arrhenius equation is expressed by the following equation:

$$k = A_f e^{-E_a/RT} \quad (4)$$

where A_f is the pre-exponential factor.

Now k in Equation (3) is substituted in Equation (4) and after considering logarithm transformation, Equation (3) can be rewritten as:

$$\ln (dQ/dt) = \ln (CA_f[B]^l[E]^m[A]^n) - E_a/RT \quad (5)$$

The first terms on the right side of Equation (5) can be considered as constant at initial cure time taken to be at $(dQ/dt)_{\max}$.^[14] The value of torque is relatively low before $(dQ/dt)_{\max}$ and this region generally corresponds to an induction period. Therefore, E_a of the vulcanizate was calculated from the slope of $\ln dQ/dt_{\max}$ versus $1/T$ plot (Figure 4a). According to this method, the E_a of the ENR/AT-PDMS system was found to be $\approx 62 \text{ kJ mol}^{-1}$. Whereas, this value for the ENR50 sulfur vulcanizate was estimated to be in the lower range of $36\text{--}52 \text{ kJ mol}^{-1}$ obtained at different vulcanization temperature.^[30] The higher activation energy of the ENR/AT-PDMS system as compared with the ENR-sulfur vulcanizate is reflected from the longer curing period of the AT-PDMS based system. (Figure 2c).

The order of the curing reaction of ENR/AT-PDMS system with respect to amine was also estimated. The Equation (3) can be expressed in the following manner:

$$\ln (dQ/dt) = \ln CK[B]^l[E]^m + n \ln [A] \quad (6)$$

Here, rate of curing reaction was calculated from the slope of $\ln(dQ/dt)_{\max}$ versus $\ln[A]$ plot (Figure 4b). The slope, n was calculated to be ≈ 0.95 suggesting that the curing reaction was first order with respect to amine concentration in the AT-PDMS. In accord with the present finding, a similar first-order curing reac-

tion of ENR with *p*-phenylenediamine catalyzed by bisphenol A was reported.^[13]

To compare ENR/AT-PDMS curing system with a typical sulfur-based curing formulation, another set of reference experiment was carried out with a standard sulfur curing system (Table 1b). In an isothermal time sweep mode at $160 \text{ }^\circ\text{C}$, a higher value of maximum torque in the ENR/AT-PDMS curing system was observed compared to the sulfur-based curing system. On the other hand, sulfur-based curing systems were tended to reversion at a higher time scale due to the cleavage of polysulphide linkages in the network. In contrast, a steady-state increment of torque was achieved for ENR/AT-PDMS system, suggesting a more robust and stable crosslinked network structure.

The crosslink density values of ENR/AT-PDMS vulcanizates obtained by the equilibrium swelling method are shown in Figure 2d. At a fixed amount of hydroquinone (10 phr), crosslink density of ENR/AT-PDMS system increased with increasing AT-PDMS loading up to 20 phr and then found to decrease at 30 phr loading (Figure 2d). The highest crosslink density of 20 phr AT-PDMS loaded composition suggested high reactivity of AT-PDMS with ENR in this particular composition. On the other hand, ENR-hydroquinone system showed a lower crosslink density value indicating low reactivity of hydroquinone with ENR. Interestingly, crosslinked density of ENR sulfur curing system was found to be lower than the ENR/AT-PDMS system (Figure 2d).

The ENR curing reactions with hydroquinone and AT-PDMS can be detected to some extent from the FTIR Spectra. A straightforward comparison among pure ENR, ENR-HQ, and ENR-PDMS-HQ systems can be observed (Figure 5a,b). The peak at 879 cm^{-1} is related to stretching vibration of epoxy ring in the main ENR chain.^[31] This peak was shifted to lower wavenumbers, 870 and 867 cm^{-1} , respectively, when ENR was cured with hydroquinone and hydroquinone-AT PDMS mixer, respectively. This suggested a ring-opening reaction of epoxy group of ENR with hydroquinone and AT-PDMS, respectively. Furthermore, it can be seen that in pure ENR a broad peak at 1110 cm^{-1} was appeared due to hydrogen bonding related to tetrahydrofuran ring.^[32] This tetrahydrofuran is a side reaction product that generally exists for a higher epoxy-group containing ENR that

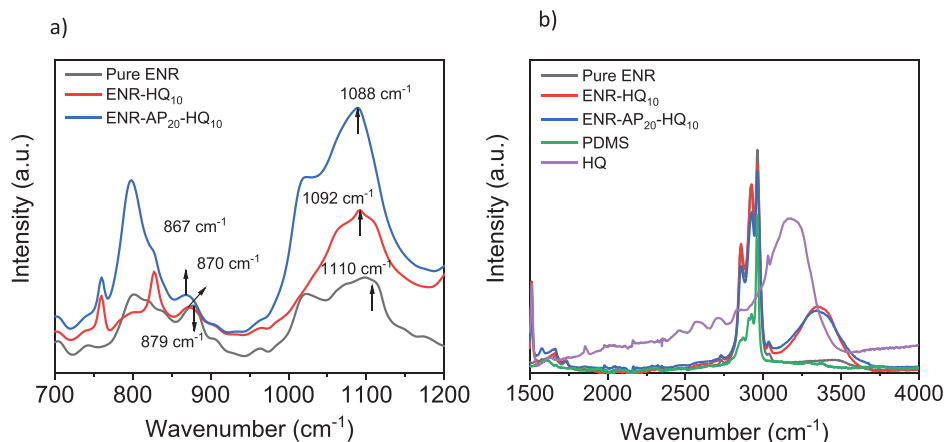


Figure 5. FTIR analysis of different compounds: a) comparison between pure ENR with ENR/HQ and ENR/HQ/PDMS systems, b) comparison among, pure ENR, HQ, and PDMS with ENR/HQ and ENR/HQ/PDMS systems.

can undergo ring-opening reactions.^[32] Interestingly, this peak was also sifted to lower wavenumbers. This might result from disruption of hydrogen bonding by adding hydroquinone and hydroquinone-AT PDMS mixer, respectively. The reaction of the amine group of PDMS with epoxy groups of ENR should have been found from FTIR from the change of the asymmetrical and the symmetrical N–H stretching bands of primary and secondary amines. However, the FTIR spectrum (Figure 5b) AT-PDMS did not show the characteristics of stretching bands of amine functionality. The reason could be due to the presence of a minimum of amine in AT-PDMS.^[24] Thus, the reaction of amines with epoxy groups of ENR could not be evident from FTIR; the only ring opening reaction of epoxy is apparent from the FTIR results.

Temperature scanning stress relaxation (TSSR) experiments were carried out by monitoring the non-isothermal relaxation behavior as a function of temperature to better understand the ENR crosslinking process by AT-PDMS, hydroquinone, and sulfur, respectively. Mechanical stress relaxation behavior of elastomeric materials is of great significance when considering these kinds of new materials under several service conditions. The mechanical stress according to theory of rubber elasticity can be expressed by the following Neo–Hookean equation:^[33]

$$\sigma = \nu RT (\lambda - \lambda^{-2}) \quad (7)$$

where ν is the crosslink density, λ is the strain ratio, and R is the universal gas constant.

When considering the temperature dependence of the strain, Equation (1) can be expressed in the following form:

$$\sigma = \nu RT \left[\frac{\lambda_0}{1 + \alpha \Delta T} - \left(\frac{\lambda_0}{1 + \alpha \Delta T} \right)^{-2} \right] \quad (8)$$

where α is the coefficient of linear thermal expansion and λ_0 is the initial strain ratio at temperature T_0 .

In the TSSR experiment, at a constant λ value, sample temperature is increased with a constant heating rate. The relaxation

spectrum at constant heating rate and at a constant λ can be calculated from the following equation:^[27]

$$H = -T \left(\frac{dE_{\text{non-iso}}(T)}{dT} \right) \quad (9)$$

where $E_{\text{non-iso}}$ is the non-isothermal relaxation modulus. It can be possible to observe the entire relaxation spectrum within a relative short period during a temperature scan due to strong temperature dependence of the relaxation time.

The isothermal relaxation measurements (at 23 °C) of different ENR vulcanizates are shown in Figure 6a,b. The reduction of isothermal stress and relative stress with time was prominent for the ENR-S system. The change of stress with time is minimal for both ENR-PDMS and ENR-HQ systems. The amine-cured ENR network is more stable than the sulfur network. The decrease of stress in the sulfur network is associated with the cleavage of some of the polysulphide linkages.

Thermal stability of the elastomer network is an essential property of rubber vulcanizates. A substantial decrease of stress with temperature is generally associated with the rubber network's thermal degradation (Figure 6c). Significant peaks that appear in the relaxation spectrum suggest the temperature at which cleavage of the crosslinks or scission of the main chains occurs. At the same time each peak reflects a specific relaxation mechanism. Relaxation spectra of different ENR vulcanizates obtained from TSSR measurements are shown in Figure 6d. In case of the ENR-PDMS system, a prominent peak at temperature >200 °C might be associated with the cleavage of amine networks which is more thermally stable and need higher temperature to be damaged. This peak was shifted to lower temperature ≈ 190 °C for the ENR-HQ vulcanizate associated with the cleavage of hydroquinone network. However, a less prominent peak at ≈ 55 °C was also evident for ENR-HQ vulcanizate, the origin of which cannot be explained. On the other hand, for the ENR-S vulcanizate the peak appeared at a relatively lower temperature (≈ 140 °C) compared to the ENR-PDMS and ENR-HQ systems. This is due to the cleavage of sulfur bridges and networks. Also, a sharper decrease in the relative stress with temperature for the ENR-S vulcanizate compared to the ENR-PDMS and ENR-HQ systems suggested

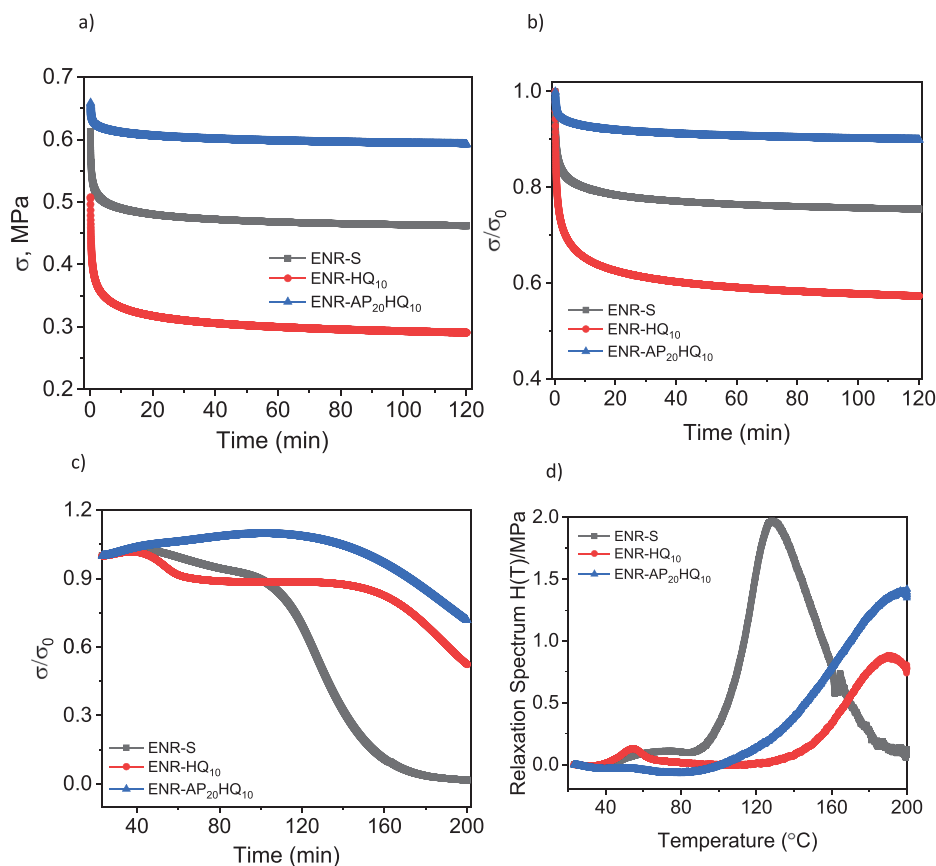


Figure 6. The isothermal stress versus time plots, b) relative stress versus time plots, c) non-isothermal relative stress versus temperature, and d) relaxation spectrum versus temperature plots of ENR-S, ENR/HQ, and ENR/PDMS/HQ systems.

faster thermal degradation of the sulfur network. Therefore, ENR/PDMS networks exhibited higher thermal stability than the ENR-sulfur system. The effect of AT-PDMS and hydroquinone on the mechanical properties of the resultant vulcanizates was investigated. With an increase in AT-PDMS loading up to 20 phr, progressive increase in modulus at 100% elongation, tensile strength, and elongation at break were found (Figure 7a). However, at 30 phr loading of AT-PDMS, a reduction in tensile strength and elongation at break was observed. This could be correlated with the decrease in crosslinked density in the 30 phr AT-PDMS loaded composition, as discussed earlier. Tensile properties of ENR-hydroquinone system were inferior due to the formation of a weak crosslink network, as evident from its low crosslink density value. Significant enhancement of tensile properties was obtained when AT-PDMS was used along with hydroquinone. Interestingly, 20 phr AT-PDMS loaded ENR with a fixed amount of hydroquinone (10 phr) showed the highest tensile strength and elongation at break. Tensile properties of the optimized composition (ENR/15Si/10HQ/20AT-PDMS) were compared with a typical ENR sulfur system (Figure 7b,c). Under the same curing conditions, ENR/AT-PDMS system showed higher tensile strength and elongation at break with lower moduli (at 100%, 200%, and 300% elongation, respectively) and hardness when compared with the typical ENR sulfur system. The shore A hardness, modulus at 100% elongation,

and elongation at break of ENR/AT-PDMS were ≈ 39 , ≈ 0.8 MPa, and $\approx 630\%$. These values were ≈ 45 , ≈ 1.0 MPa, and $\approx 520\%$ for the ENR sulfur system. This suggested that the ENR/AT-PDMS vulcanizate is more stretchable and less rigid than the standard ENR sulfur system. Despite a relatively higher crosslink density in the ENR/AT-PDMS vulcanizate than ENR sulfur system, the higher elongation at break and lower hardness and modulus is attributed to the soft and flexible PDMS chains in the resulting elastomer networks.

The cyclic uniaxial tensile stress–strain curves with different strains 50%, 100%, and 150% are shown in Figure 7c. Both the ENR-sulfur and ENR/AT-PDMS cross-linked system exhibited a typical stress-induced softening effect with hysteresis and permanent residual strain behavior. The stress-softening behavior of the ENR-sulfur system is comparatively more prominent than the ENR/AT-PDMS system in each cycle because of the quasi-irreversible rearrangements of the mono-, di-, and poly sulphidic linkages in the ENR sulfur network during stretching and deformation. A comparatively smaller hysteresis loop was observed for the ENR/AT-PDMS system than the ENR-sulfur system. Dynamic mechanical analysis of the ENR/AT-PDMS system measured under temperature sweep conditions is shown in Figure 8a,b. At elevated temperatures (30–100 °C), storage modulus (E') was found to increase with an increase in AT-PDMS loading. Also, in the rubbery plateau region, the reduction of E'

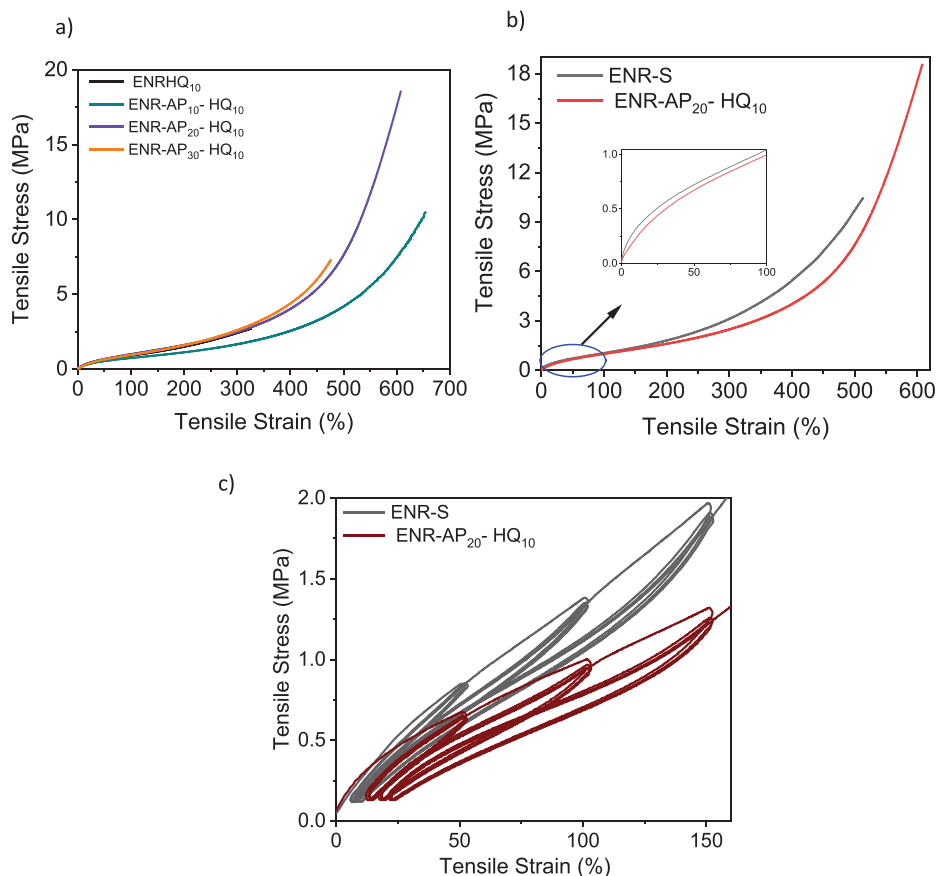


Figure 7. a) Uniaxial tensile stress versus tensile strain of ENR/AT-PDMS system with various amounts of AT-PDMS. Highest value of tensile strength and elongation at break was obtained at 20 phr AT-PDMS loading. b) Comparison of tensile properties of the optimum ENR/AT-PDMS system (ENR/10HQ/20AT-PDMS) with a typical ENR-sulfur system. Inset is the comparison of modulus at 100% elongation. c) Comparison of cyclic uniaxial tensile stress–strain curves with different strains of 50%, 100%, and 150% of the optimum ENR/AT-PDMS system (ENR/10HQ/20AT-PDMS) with a typical ENR-sulfur system.

for lower AT-PDMS loaded compositions (2.5 and 5 phr, respectively) was attributed to their lightly crosslinked networks, which are evident from lower crosslinked density values (Figure S2a). ENR/AT-PDMS system networks exhibited two glass transition temperatures (T_g), -1 and -120 °C, which correspond to ENR and PDMS phases, respectively (Figure 8b). This suggested the formation of a hybrid elastomeric network structure in the resultant materials. However, T_g of PDMS phase was not observed for lower AT-PDMS loaded compositions, 2.5 and 5 phr, respectively (Figure S2b). Interestingly, upon an increase in the AT-PDMS loading, T_g of ENR phase was slightly shifted toward lower temperature, with a slight reduction of $\tan\delta$ peak height at the T_g of ENR. The shifting of T_g can be attributed to the soft and highly flexible PDMS chains, while reduction of $\tan\delta$ height can be correlated with increased crosslinked density.

Dynamic mechanical properties of the optimized composition, that is, 20 phr loaded AT-PDMS (ENR/15Si/10HQ/20AT-PDMS) were compared with a standard ENR sulfur system (Figure 8a,b). In the glassy region, E' of ENR/AT-PDMS system was lower than ENR-S system. Besides, at room temperature, the ENR/AT-PDMS system showed a lower E' value than the ENR-S system. The values of E' were ≈ 2.9 and ≈ 4.9 MPa for ENR/AT-

PDMS and ENR-S system, respectively. Interestingly, in the rubbery plateau region, slight enhancement of E' was observed for ENR/AT-PDMS system compared to the ENR-S system. This can be correlated with a relatively more robust and stable crosslinked network system for amine cured ENR than a conventional S cured system.

Understanding of the dynamic mechanical properties of polymeric materials over a wide range of frequencies is crucial for their application point of view.^[34] The mechanical behavior of ENR/AT-PDMS system over various frequency regimes, such as glassy regime at very high frequencies, followed by Rouse regime at the intermediate frequencies and low-frequency regime, were measured and compared with a typical ENR sulfur system. Mechanical relaxation of lightly crosslink rubber at a lower frequency regime is associated with slow reptation dynamics of dangling chains. The influence of such relaxation dynamics of both the networks at lower frequencies was compared. There was a marginal difference in the storage and loss moduli and loss tangent of both the ENR/AT-PDMS and ENR-S system (Figure 8c,d) at higher frequencies. A change of the slope was observed in the storage modulus plot, and a power-law frequency behavior is evident in the intermediate frequencies. The ENR/AT-PDMS/HQ

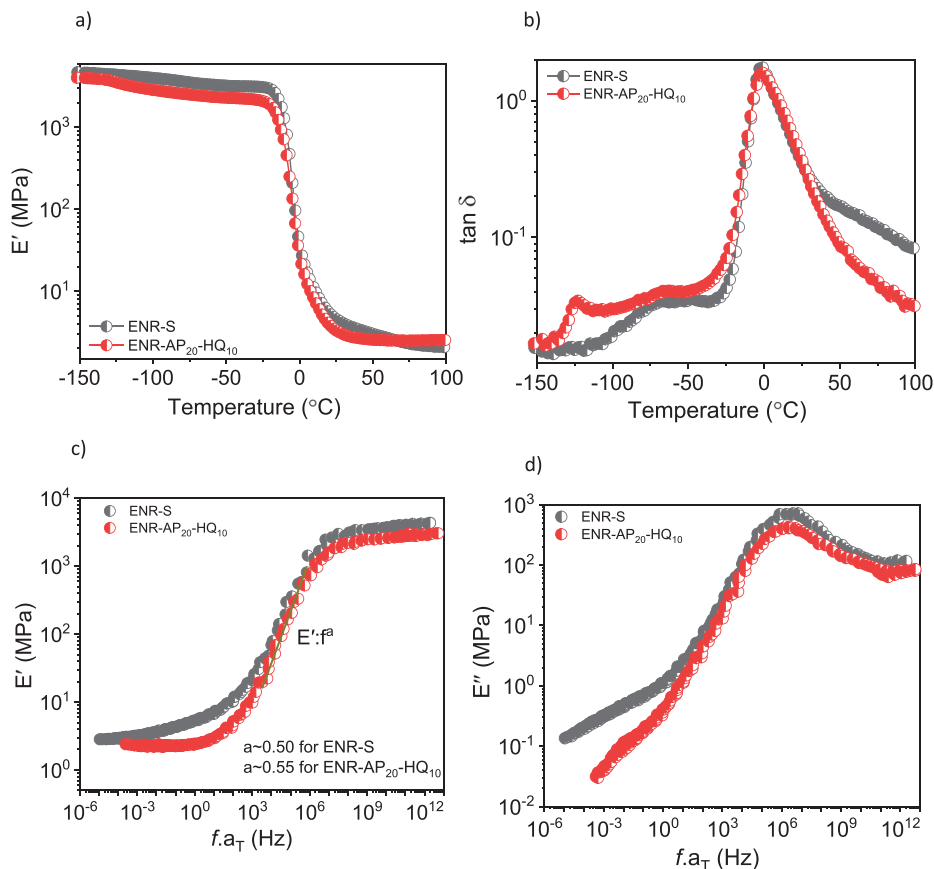


Figure 8. a,b) Log scale plot of storage modulus (E') and loss tangent ($\tan\delta$) versus temperature of the optimum ENR/AT-PDMS system (ENR/15Si/10HQ/20AT-PDMS) and with a typical ENR-sulfur system. c,d) Comparison of TTS-derived frequency dependence storage modulus (E') and loss modulus (E'') master curves of the optimum ENR/AT-PDMS system (ENR/10HQ/20AT-PDMS) with a typical ENR-sulfur system. Both of the axes are in log scale.

system's slope is $E' \propto f^{0.56}$, whereas, for ENR-S, a slightly different value with $E' \propto f^{0.50}$ was obtained, reflecting the Rouse-like regime. The steeper slope in ENR/AT-PDMS/HQ system can be correlated with restricted movement of the semiflexible chains by chemical linkage of the chain segments.^[35] It is well known that the dynamic moduli at the higher and intermediate-frequency regions remain unaffected by the crosslink density of networks. The network chains between crosslink in these regimes can only undergo slight sliding motions, which cannot significantly

affect the dynamic moduli and, thus, are cross-link density-independent.^[36] However, dynamic moduli (storage modulus and loss modulus) of the ENR/AT-PDMS system were lower than the ENR-S system at the low-frequency range. At lower frequencies, the polymer network's storage modulus tends to the value of the plateau modulus from mechanically active network strands between network junctions. The values of plateau modulus were ≈ 2.8 and ≈ 2.2 MPa for the ENR/AT-PDMS and ENR-S system, respectively. The dynamic mechanical response at low-frequency

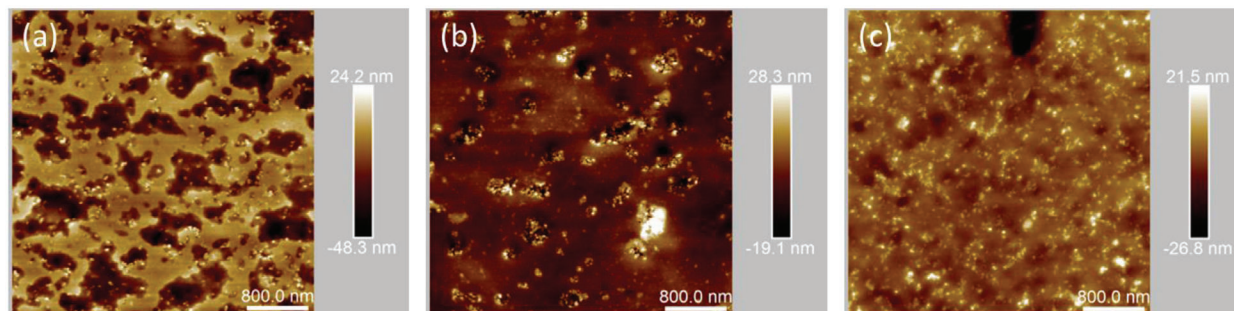


Figure 9. AFM image of a) ENR/15Si/10HQ/5AT-PDMS system. b) AFM image of ENR/10HQ/20AT-PDMS system. c) AFM image of ENR-S system.

generally originated from the collective motion of chains from a network structure and depends on crosslink density of network. However, crosslinked density of the ENR/AT-PDMS/HQ system was higher than the ENR-S system. Therefore, at lower frequencies, lower dynamic moduli of ENR/AT-PDMS system can be attributed to the soft and highly flexible PDMS chains. Additionally, the nature of crosslinking structures is different for both systems. **Figure 9a–c** shows the AFM images of the silica filled ENR/AT-PDMS and ENR-S vulcanizates. AFM was carried out to investigate the phase structure of ENR and AT-PDMS. In the case of ENR/AT-PDMS vulcanizate, the appearance of the two phases, ENR and PDMS were apparent, where PDMS was dispersed in the ENR matrix. A sea–iceland type morphology was observed (Figure 9a). However, the dispersion of silica is not uniform, and some agglomerated silica structures appeared in the ENR/AT-PDMS vulcanizate (Figure 9a,b). On the other hand, the dispersion of silica was comparatively uniform in the ENR matrix in the case of ENR-S vulcanizate (Figure 9c).

4. Conclusions

The feasibility of curing ENR with a low molecular weight AT-PDMS in the presence of hydroquinone was explored for the first time to develop soft and highly stretchable hybrid elastomeric materials. The hybrid elastomeric network structure of the resultant material was demonstrated from its two glass transition temperatures, -1 and -120 °C which corresponded to the ENR and PDMS phases, respectively. A combination of 20 phr AT-PDMS and 10 phr hydroquinone in the ENR formulation offered a substantial improvement in torque value which is indicating a well state of crosslinking network. The high reactivity of AT-PDMS with epoxy group of ENR was probably originated from enhanced nucleophilicity of the amine group when catalyzed by hydroquinone. The apparent activation energy of the ENR/AT-PDMS vulcanizate was found to be ≈ 62 kJ mol $^{-1}$ and the curing reaction was found to be first order with respect to the amine concentration. Interestingly, ENR/AT-PDMS vulcanizate was found to be more stretchable and soft at room temperature as compared to a typical ENR-sulfur vulcanizate. The shore A hardness, modulus at 100% elongation and elongation at break of the ENR/AT-PDMS vulcanizate were ≈ 38 , ≈ 0.8 MPa, and $\approx 630\%$, respectively. These values were ≈ 45 , ≈ 1.0 MPa, and $\approx 520\%$ for the ENR sulfur vulcanizate. However, the most striking feature of the AT-PDMS system that the tensile strength reaches to the value of nearly 19 MPa and for sulfur system it is only 10 MPa. The nature of crosslinking structures was evaluated from the non-isothermal mechanical relaxation process. ENR/AT-PDMS network structure was thermally more stable than ENR-sulfur system. Despite the relatively higher crosslink density in the ENR/AT-PDMS vulcanizate as compared to ENR sulfur system, the higher stretchability in terms of elongation at break, and lower hardness and modulus in this vulcanizate was originated from the introduction of soft and highly flexible PDMS chains by curing process in the resulting elastomer networks. Beyond an interest in elastomer, this efficient yet simple crosslinking system using liquid AT-PDMS may find a use in the material development in a more general field of soft materials technology.

Supporting Information

Supporting Information is available from the Wiley Online Library or from the author.

Acknowledgements

The corresponding work was financially supported by The Deutsche Forschungsgemeinschaft (DFG, German Research Foundation) project ID 330167-SPP 2100. G.H. acknowledges the DFG (German Research Foundation) project 380321452/GRK2430 for financial support.

Open access funding enabled and organized by Projekt DEAL.

Conflict of Interest

The authors declare no conflict of interest.

Data Availability Statement

Research data are not shared.

Keywords

epoxidized natural rubber, hybrid elastomer networks, mechanical properties, polydimethylsiloxane

Received: May 26, 2021
Revised: August 3, 2021
Published online: August 21, 2021

- [1] M. Pire, C. Lorthioir, E. K. Oikonomou, S. Norvez, I. Iliopoulos, B. Le Rossignol, L. Leibler, *Polym. Chem.* **2012**, *3*, 946.
- [2] S.-N. Gan, Z. A. Hamid, *Polymer* **1997**, *38*, 1953.
- [3] A. Mousa, U. S. Ishiaku, Z. A. M. Ishak, *J. Appl. Polym. Sci.* **1998**, *69*, 1357.
- [4] M. d. A. Rhaman, M. Penco, G. Spagnoli, A. M. Grande, L. Di Landro, *Macromol. Mater. Eng.* **2011**, *296*, 1119.
- [5] D. J. Lowe, A. V. Chapman, S. Cook, J. J. C. Busfield, *Macromol. Mater. Eng.* **2011**, *296*, 693.
- [6] X. Zhang, K. Niu, W. Song, S. Yan, X. Zhao, Y. Lu, L. Zhang, *Macromol. Rapid Commun.* **2019**, *40*, 1900042.
- [7] S. N. Koklas, D. D. Sotiropoulou, J. K. Kallitsis, N. K. Kalfoglou, *Polymer* **1991**, *32*, 66.
- [8] S. Salaeh, G. Boiteux, O. Gain, P. Cassagnau, C. Nakason, *Adv. Mater. Res.* **2014**, *844*, 97.
- [9] S. S. Banerjee, S. Hait, T. S. Natarajan, S. Wießner, K. W. Stöckelhuber, D. Jehnichen, A. Janke, D. Fischer, G. Heinrich, J. J. Busfield, A. Das, *J. Phys. Chem. B* **2019**, *123*, 5168.
- [10] M. R. Krejsa, J. L. Koenig, *Rubber Chem. Technol.* **1993**, *66*, 376.
- [11] M. Pire, S. Norvez, I. Iliopoulos, B. Le Rossignol, L. Leibler, *Polymer* **2011**, *52*, 5243.
- [12] C. T. Ratnam, S. Kamaruddin, Y. Sivachalam, M. Talib, N. Yahya, *Polym. Test.* **2006**, *25*, 475.
- [13] A. S. Hashim, S. Kohjiya, *J. Polym. Sci., Part A: Polym. Chem.* **1994**, *32*, 1149.
- [14] A. S. Hashim, S. Kohjiya, *Polym. Gels Networks* **1994**, *2*, 219.
- [15] R. N. Kumar, R. Mehnert, *Macromol. Mater. Eng.* **2001**, *286*, 449.
- [16] A. Hillerström, B. Kronberg, *J. Appl. Polym. Sci.* **2008**, *110*, 3059.

- [17] S. Shankar Banerjee, I. Ramakrishnan, B. K. Satapathy, *Polym. Eng. Sci.* **2017**, 57, 973.
- [18] S. S. Banerjee, I. Ramakrishnan, B. K. Satapathy, *Polym. Eng. Sci.* **2016**, 56, 491.
- [19] G. J. Price, I. M. Shillcock, *J. Chromatogr. A* **2002**, 964, 199.
- [20] J.-E. Ehlers, N. G. Rondan, L. K. Huynh, H. Pham, M. Marks, T. N. Truong, *Macromolecules* **2007**, 40, 4370.
- [21] J. Mijovic, A. Fishbain, J. Wijaya, *Macromolecules* **1992**, 25, 979.
- [22] E. J. Markvicka, M. D. Bartlett, X. Huang, C. Majidi, *Nat. Mater.* **2018**, 17, 618.
- [23] N. Lu, D.-H. Kim, *Soft Rob.* **2014**, 1, 53.
- [24] S. S. Banerjee, S. Mandal, I. Arief, R. K. Layek, A. K. Ghosh, K. Yang, J. Kumar, P. Formanek, A. Fery, G. Heinrich, A. Das, *ACS Appl. Mater. Interfaces* **2021**, 13, 15610.
- [25] D. Basu, A. Das, K. W. Stöckelhuber, D. Jehnichen, P. Formanek, E. Sarlin, J. Vuorinen, G. Heinrich, *Macromolecules* **2014**, 47, 3436.
- [26] W. G. Hwang, K. H. Wei, C. M. Wu, *Polym. Eng. Sci.* **2004**, 44, 2117.
- [27] S. S. Banerjee, T. S. Natarajan, E. Subramani B, S. Wießner, A. Janke, G. Heinrich, A. Das, *J. Appl. Polym. Sci.* **2020**, 137, 48344.
- [28] R. Hamzah, M. A. Bakar, O. S. Dahham, N. N. Zulkepli, S. S. Dahham, *J. Appl. Polym. Sci.* **2016**, 133, 44123.
- [29] M.-P. Pham, *Theoretical Studies of Mechanisms of Epoxy Curing Systems*, The University of Utah, **2011**.
- [30] B. T. Poh, B. K. Tan, *J. Appl. Polym. Sci.* **1991**, 42, 1407.
- [31] Y. Zhang, H. Li, C. Li, X. Chen, A. Lesser, *Polym. Eng. Sci.* **2019**, 59, E367.
- [32] X. Zhang, Z. Tang, B. Guo, L. Zhang, *ACS Appl. Mater. Interfaces* **2016**, 8, 32520.
- [33] L. R. G. Treloar, *The Physics of Rubber Elasticity*, Oxford University Press, USA **1975**.
- [34] M. Saphiannikova, V. Toshchevikov, I. Gazuz, F. Petry, S. Westermann, G. Heinrich, *Macromolecules* **2014**, 47, 4813.
- [35] T. A. Vilgis, *Polymer* **2005**, 46, 4223.
- [36] A. A. Gurtovenko, Y. Ya. Gotlib, H.-G. Kilian, *Macromol. Theory Simul.* **2000**, 9, 388.